

UCLA

UCLA Previously Published Works

Title

Photogrammetry of Perfusion-Fixed Heart: Innovative Approach to Study 3-Dimensional Cardiac Anatomy.

Permalink

<https://escholarship.org/uc/item/40j257np>

Authors

Sato, Takanori
Hanna, Peter
Ajijola, Olujimi
et al.

Publication Date

2023-09-06

DOI

10.1016/j.jaccas.2023.101937

Peer reviewed

CASE REPORT

ADVANCED

CLINICAL CASE: DAVINCI CORNER

Photogrammetry of Perfusion-Fixed Heart



Innovative Approach to Study 3-Dimensional Cardiac Anatomy

Takanori Sato, MD, PhD, Peter Hanna, MD, PhD, Olujimi A. Ajijola, MD, PhD, Kalyanam Shivkumar, MD, PhD, Shumpei Mori, MD, PhD

ABSTRACT

Photogrammetry generates a 3-dimensional high-resolution model from multiple 2-dimensional photographs. Herein, we demonstrate a photogrammetry of a perfusion-fixed cardiac sample around the left ventricular summit. The single photogrammetric model can be observed from almost all directions and illustrates important anatomical features for the general cardiologist. (**Level of Difficulty: Advanced.**) (J Am Coll Cardiol Case Rep 2023;21:101937) © 2023 The Authors. Published by Elsevier on behalf of the American College of Cardiology Foundation. This is an open access article under the CC BY-NC-ND license (<http://creativecommons.org/licenses/by-nc-nd/4.0/>).

BACKGROUND AND METHODS

Photogrammetry is the applied science of generating a 3-dimensional surface-rendered reconstruction from multiple 2-dimensional photographs taken at varying angles.^{1,2} We, herein, demonstrate a

photogrammetric model of a perfusion-fixed cardiac sample. The heart rejected for transplantation was recovered from a 68-year-old male donor without structural heart disease. After removal of the epicardial fat, the sample was suspended to obtain 157 multidirectional photographs with a smartphone (**Figure 1**).³ A commercially available software application (Polycam, Polycam Inc) was used to generate the 3-dimensional model in FBX format (**Supplemental FBX file, Video 1**). The single photogrammetric model can be observed from almost all directions (3D Viewer, Microsoft) and demonstrates complex anatomical features (**Figures 1 to 18**),³⁻⁵ which is relevant to routine transcatheter cardiac procedures. Multiplanar reconstruction images of the corresponding structures obtained from clinical cardiac computed tomographic datasets of another patient without structural heart disease are presented

LEARNING OBJECTIVES

- To appreciate complementary roles of 2- and 3-dimensional imaging in clinical cardiac anatomy.
- To show that photogrammetry is a useful tool to generate 3-dimensional cardiac anatomy models from 2-dimensional images.
- To illustrate the utility of photogrammetry in cardiac anatomy from both a diagnostic and procedural standpoint.

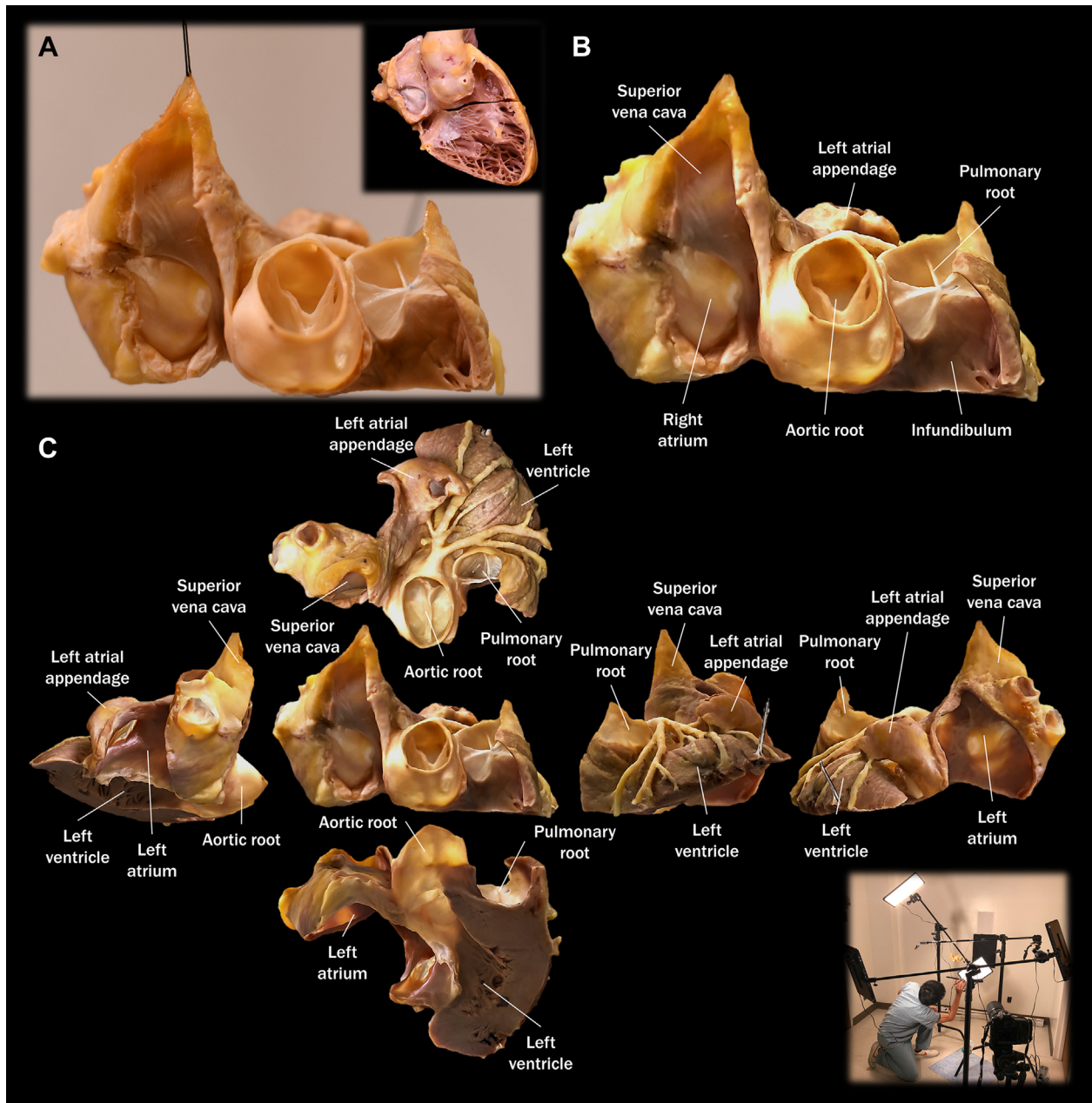
From the University of California Los Angeles (UCLA) Cardiac Arrhythmia Center, UCLA Health System, David Geffen School of Medicine at UCLA, Los Angeles, California, USA.

Nicole M. Bhavie, MD, served as Guest Associate Editor for this paper. James L. Januzzi, Jr, MD, and William Stevenson, MD, served as Guest Editor-in-Chiefs for this paper.

This paper published simultaneously in *JACC: Clinical Electrophysiology*.

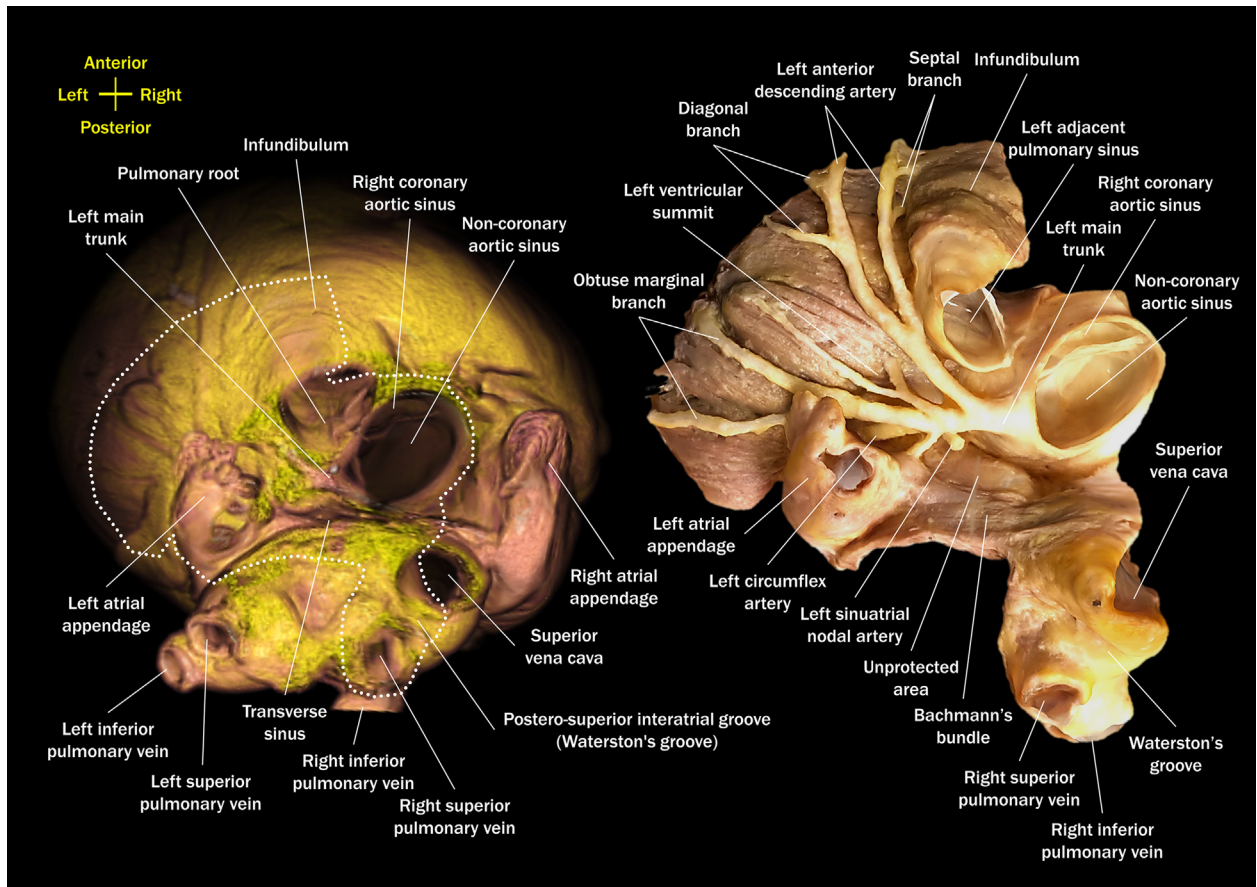
The authors attest they are in compliance with human studies committees and animal welfare regulations of the authors' institutions and Food and Drug Administration guidelines, including patient consent where appropriate. For more information, visit the [Author Center](#).

Manuscript received December 26, 2022; revised manuscript received May 4, 2023, accepted May 23, 2023.

FIGURE 1 Generation of the Photogrammetric Model

Two-dimensional photograph (A) and corresponding photogrammetric image (B) show the real and virtual cardiac specimen viewed from the right anterior oblique direction, respectively. **Inset** shows the cut plane of the heart to create the sample. The plane was nearly parallel to the inferior margin of the membranous septum,³ and the superior aspect was used for the photogrammetry after further dissection. The sample was suspended (A), and multidirectional images were taken to generate the photogrammetric model (B, C). The entire circumference of the heart sample can be observed by rotating the photogrammetric model as shown in (C). **Inset** shows our studio set-up to capture multidirectional photographs.

FIGURE 2 Topographic Location of the Sample

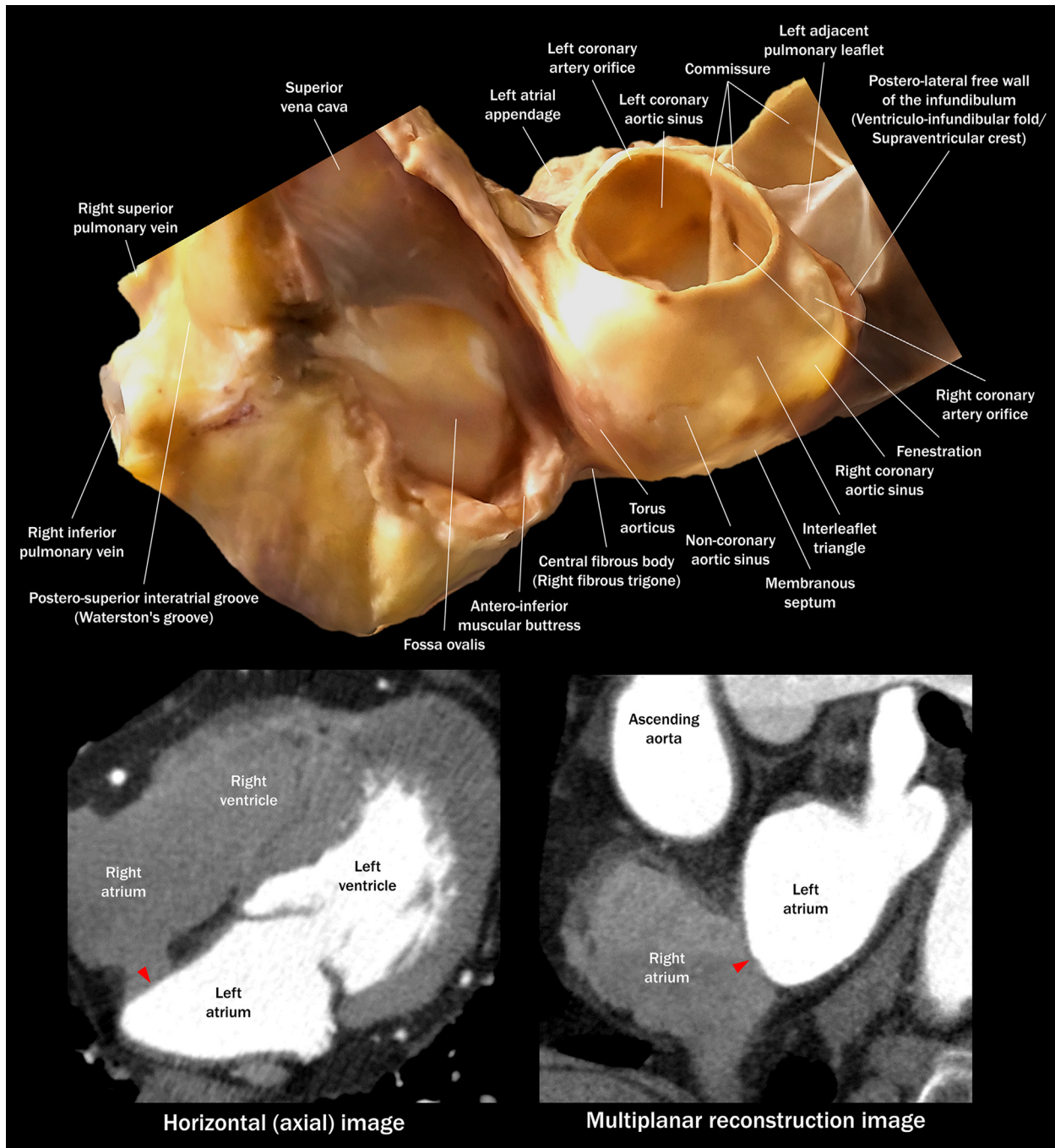


Before dissection of the heart, the whole heart underwent a computed tomographic scan (SOMATOM Definition AS, Siemens Healthcare). Virtual dissection image (**left**) is viewed from the superior aspect and is presented with a corresponding photogrammetric model (**right**). The infundibulum and pulmonary root are located left anterior to the aortic root. Both atrial appendages sandwich the arterial roots. The **white dotted line (left)** indicates the cut edge that corresponds to the sample (**right**). Epicardial fat was thoroughly removed before applying photogrammetry. The specimen includes the aortic root, left coronary artery, left ventricular summit, part of the infundibulum and pulmonary root, anterior wall of the left atrium, left atrial appendage, right pulmonary veins, and part of the superior vena cava.

together to demonstrate the complementary role of 2- and 3-dimensional learning. The STL file of this cardiac sample ([Supplemental STL file](#), [Video 2](#)) is also shared to allow readers to review the pertinent anatomy. This innovative approach may help viewers easily understand the nuances of 3-dimensional cardiac anatomy.

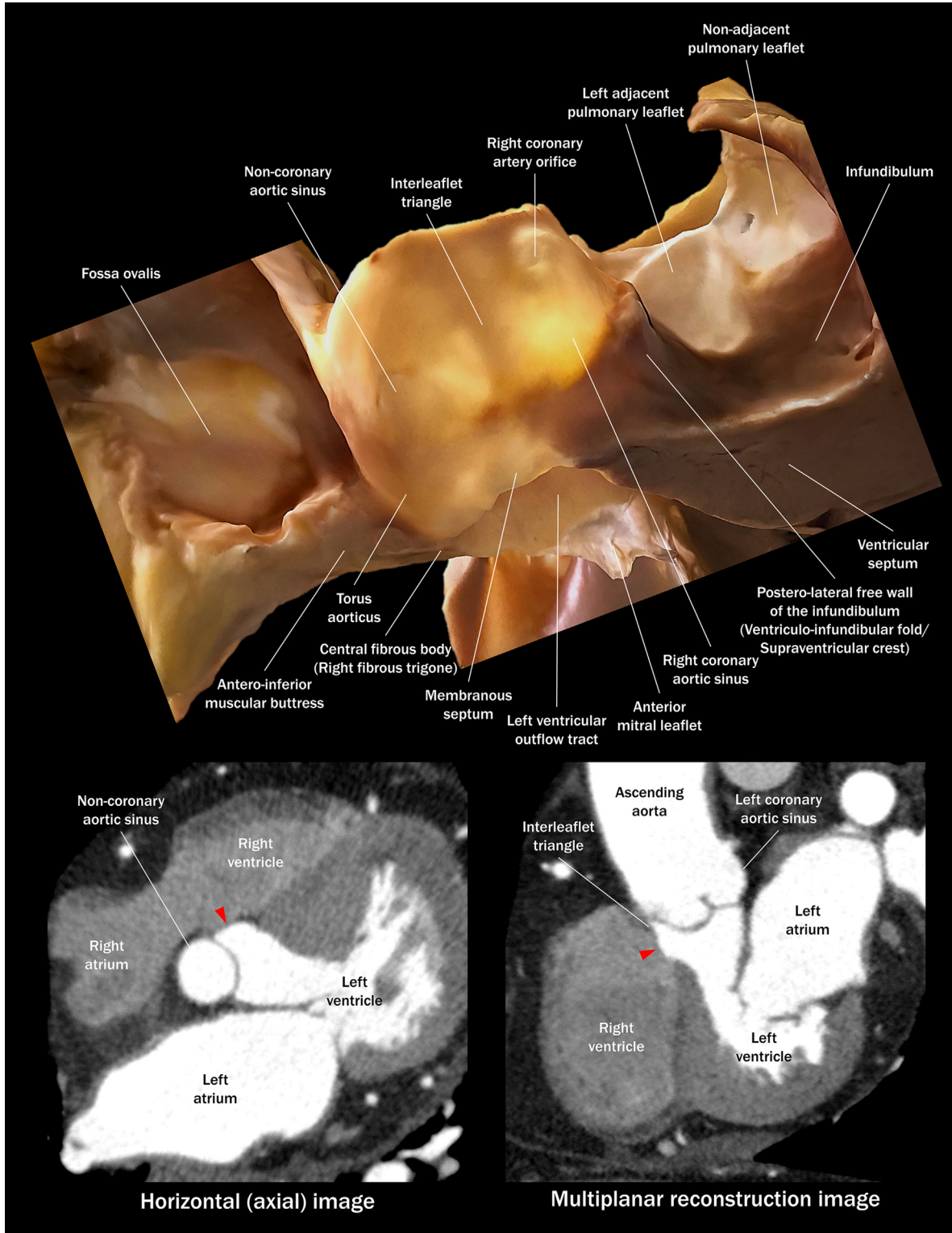
ACKNOWLEDGMENTS The authors are thankful to those individuals who have donated their bodies and tissues for the advancement of education and research. The authors thank OneLegacy Foundation

and the National Institutes of Health Stimulating Peripheral Activity to Relieve Conditions Program, which formed the basis for obtaining donor hearts for research and for funding this effort. Special thanks to Dino Pulerà and Mayandi Sivaguru for their guidance on photogrammetry. The authors are also grateful to Anthony A. Smithson and Arvin Roque-Verdeflor of the UCLA Translational Research Imaging Center (Department of Radiology) for their support in computed tomographic data acquisition. The authors appreciate our Research Operations Manager, Amiksha S. Gandhi, for her dedication to support our projects.

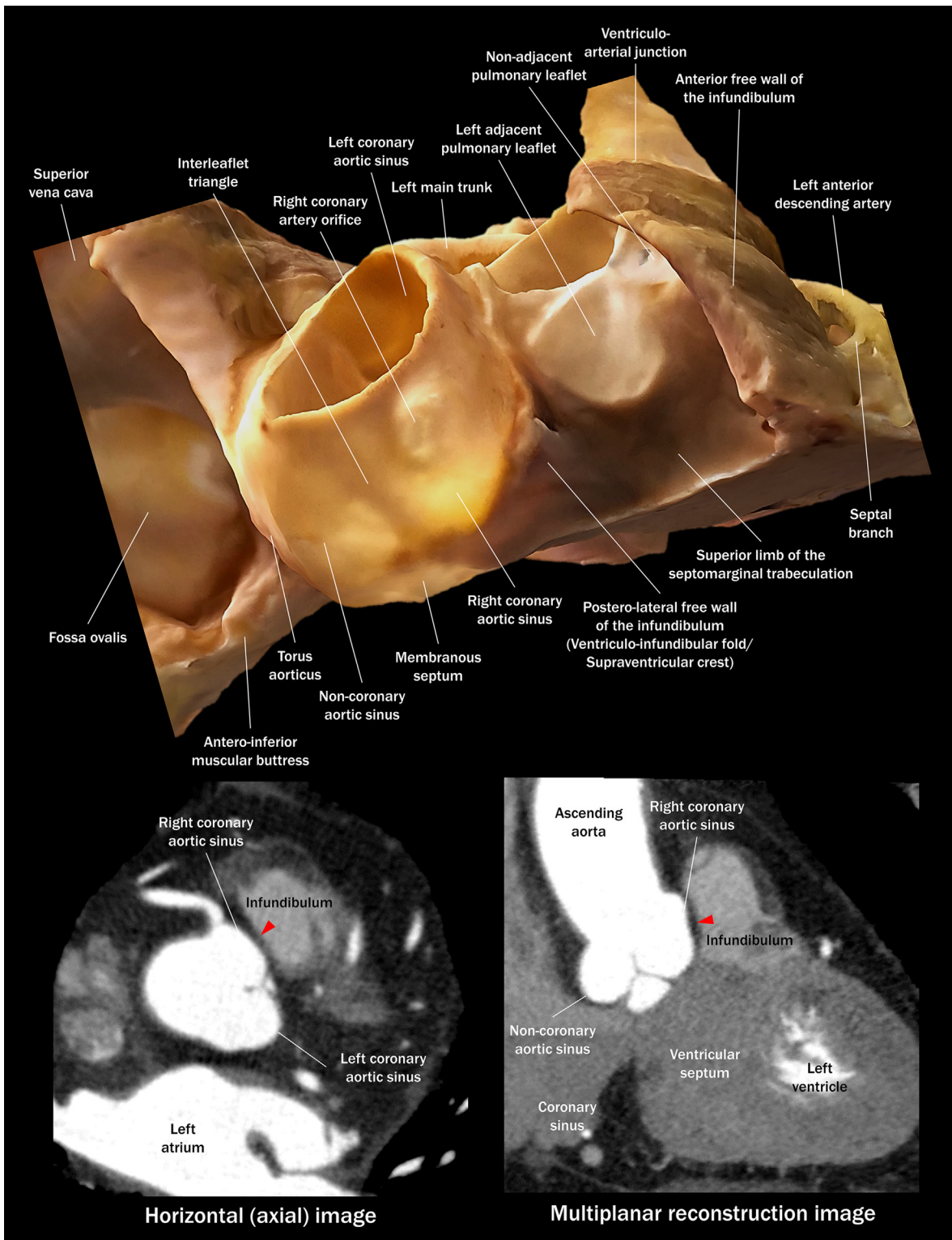
FIGURE 3 Fossa Ovalis and Torus Aorticus

The model is viewed from the steep right anterior oblique direction. The fossa ovalis is located right posterior to the noncoronary aortic sinus. It is surrounded by the interatrial grooves except for the antero-inferior muscular buttress,⁴ corresponding to the muscular true atrial septum located at the antero-inferior limbus. The right half of the noncoronary aortic sinus bulges into the right atrium, which is referred to as the torus aorticus/right aortic mound. The torus aorticus is prominent in this sample because of dilatation of the noncoronary aortic sinus. **(Bottom)** The cardiac computed tomographic images are reconstructed from the clinical case to show the fossa ovalis (**arrowheads**). These structures are relevant to atrial trans-septal catheterization, catheter ablation of atrial arrhythmia, transcatheter closure of atrial septal defect/patent foramen ovale, and transcatheter closure of aorto-right atrial fistula.

FIGURE 4 Membranous Septum

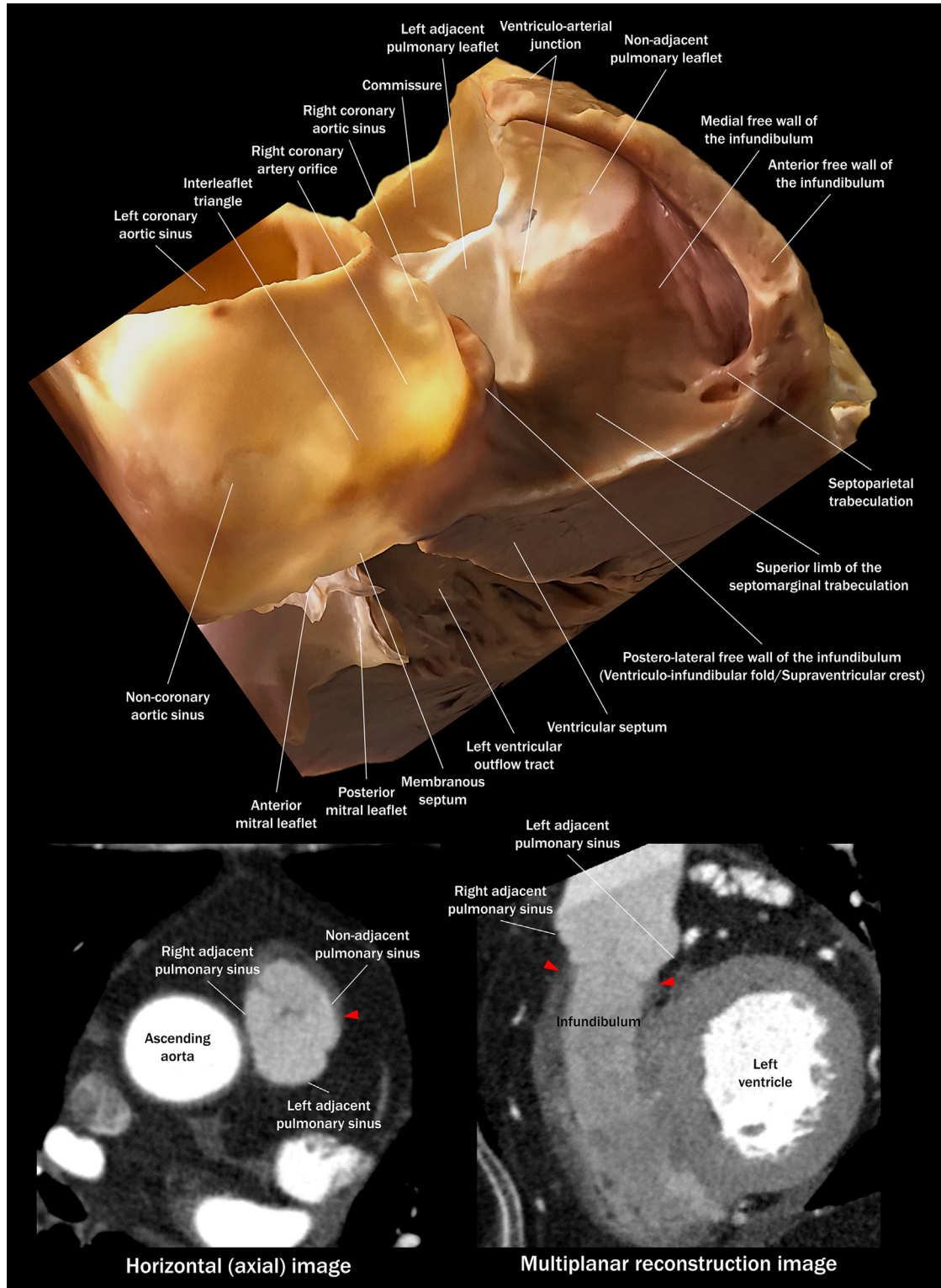


Right anterior oblique and caudal views of the model are shown. The membranous septum is located inferior to the interleaflet triangle between the non- and right coronary aortic sinuses. The membranous septum is the true anatomical septum that separates the right atrial vestibule/right ventricular inflow tract from the left ventricular outflow tract.⁴ **(Bottom)** The cardiac computed tomographic images are reconstructed from the clinical case to show the membranous septum (**arrowheads**). This structure is relevant to His-bundle pacing/left bundle branch area pacing, catheter ablation of atrial arrhythmia/para-Hisian ventricular arrhythmia/accessory pathway, catheter ablation of the atrioventricular node, transcatheter closure of the ventricular septal defect/Gerbode-type defect, transcatheter aortic valve intervention, and transcatheter tricuspid valve intervention.

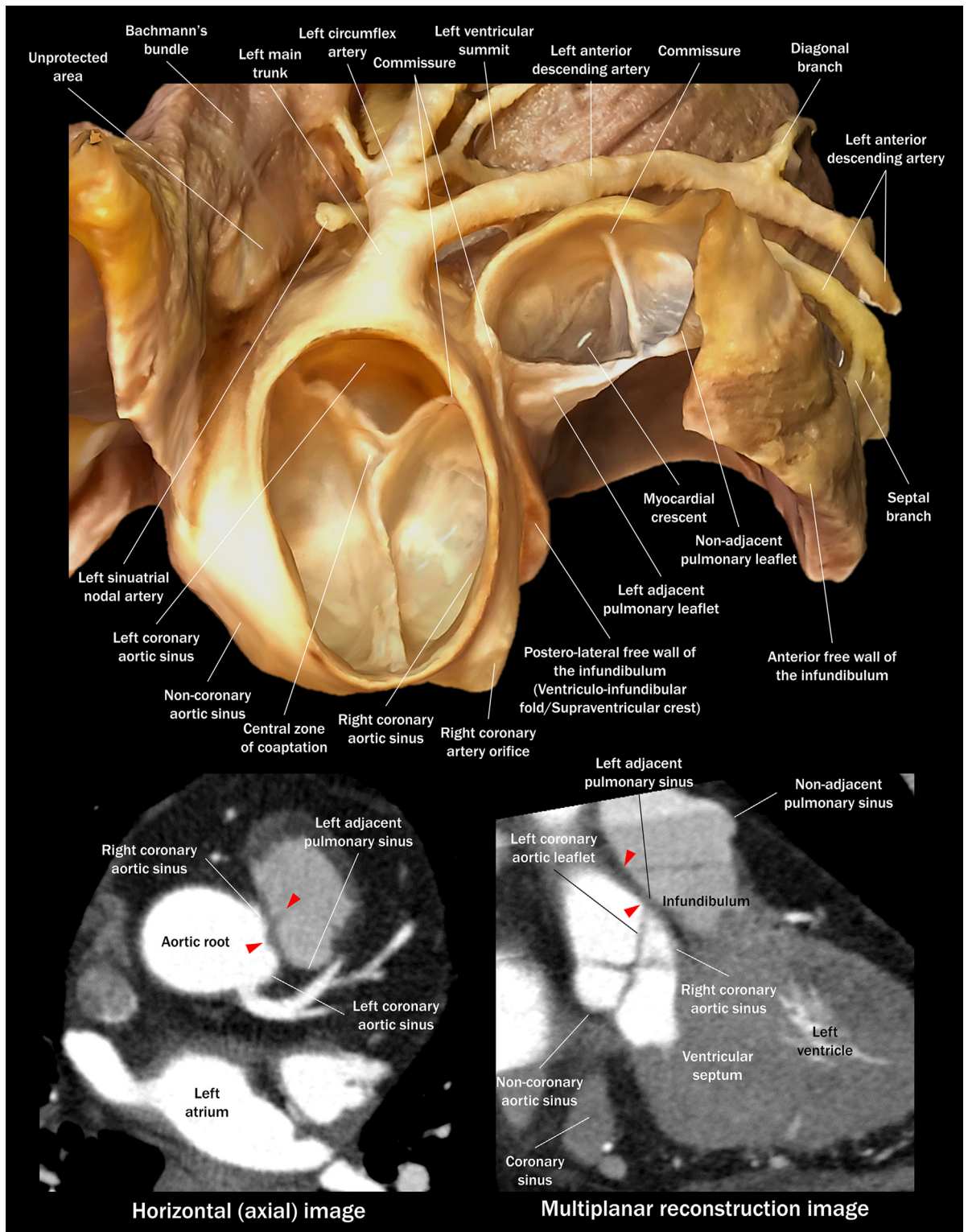
FIGURE 5 Postero-Lateral Free Wall of the Infundibulum

The model is viewed from the shallow right anterior oblique and caudal direction. The postero-lateral free wall of the infundibulum, also referred to as the ventriculo-infundibular fold, or supraventricular crest, lifts the pulmonary valve away from the tricuspid valve. The postero-lateral free wall of the infundibulum covers the right coronary aortic sinus.⁴ **(Bottom)** The cardiac computed tomographic images are reconstructed from the clinical case to show the postero-lateral free wall of the infundibulum (**arrowheads**). This structure is relevant to catheter ablation of ventricular arrhythmia, transcatheter closure of aorto-right ventricular outflow tract fistula, and transcatheter aortic valve intervention.

FIGURE 6 Ventriculo-Arterial Junction of the Pulmonary Root

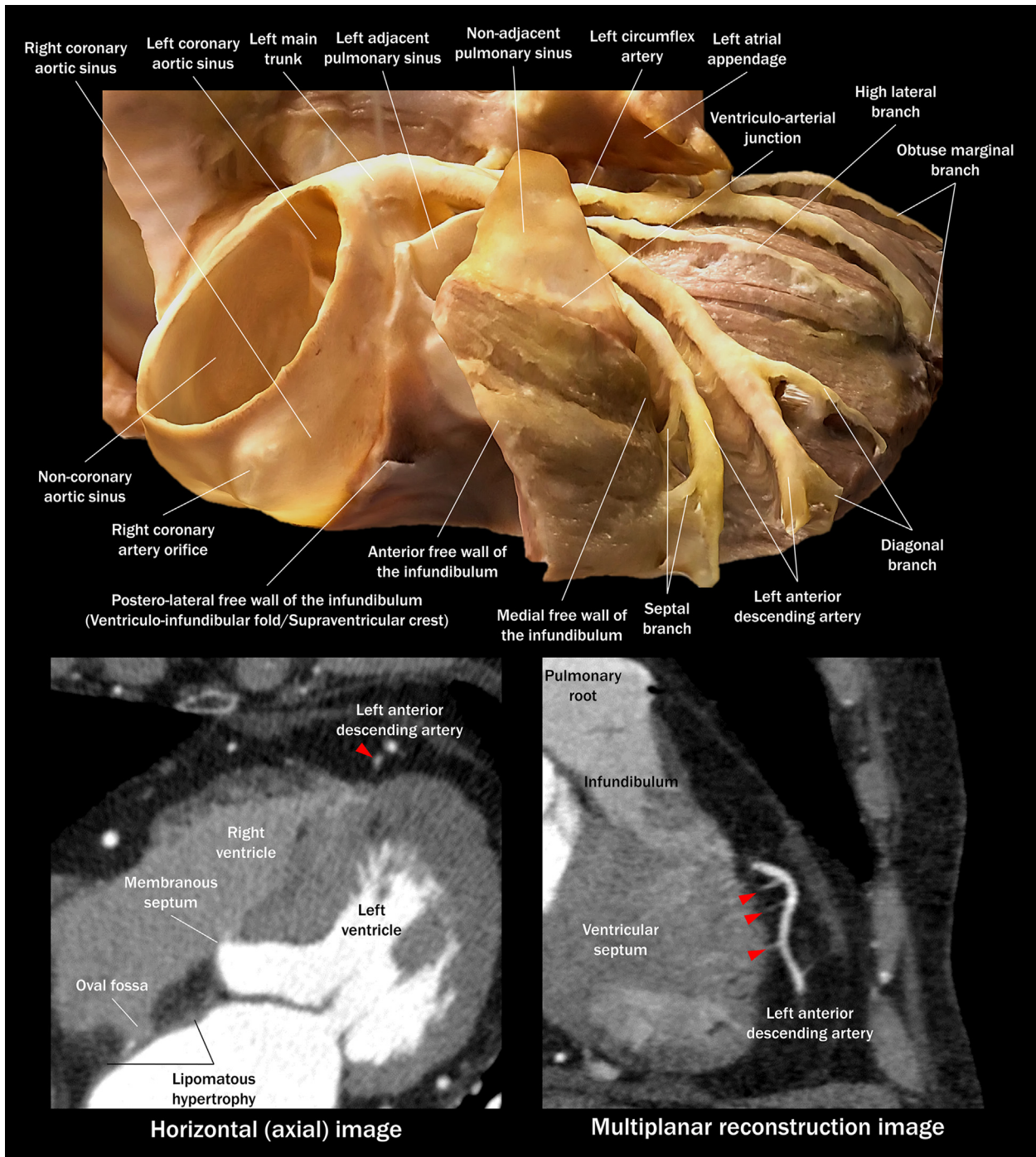


The model is viewed from the right anterior oblique and caudal direction. The ventriculo-arterial junction extends beyond the virtual basal ring of the pulmonary root.⁴ Thus, the entire circumference of the bottom of the pulmonary root is covered by the ventricular muscle of the free-standing sub-pulmonary infundibulum (Figure 9). (Bottom) The cardiac computed tomographic images are reconstructed from the clinical case to show the myocardium beneath the ventriculo-arterial junction (arrowheads), supporting the base of the pulmonary root. This structure is relevant to catheter ablation of ventricular arrhythmia and transcatheter pulmonary valve intervention.

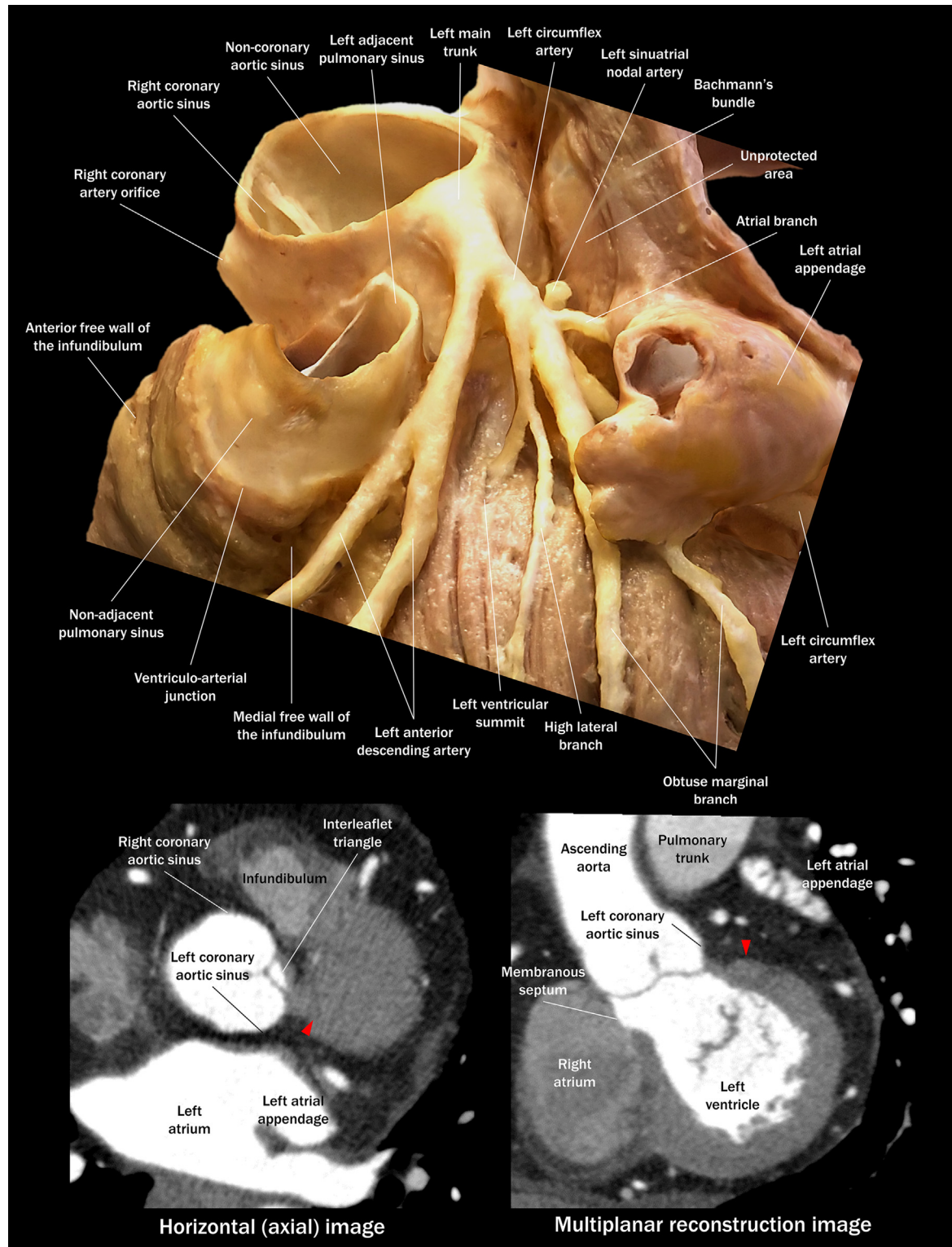
FIGURE 7 Interleaflet Triangle Between the Right and Left Coronary Aortic Sinuses

The model is viewed from the right anterior oblique and cranial direction. The apex of the interleaflet triangle between the right and left coronary aortic sinuses (commissure) and the apex of the interleaflet triangle between the right and left adjacent pulmonary sinuses (commissure) face each other,⁴ with a thin fibrous tissue interposed. **(Bottom)** The cardiac computed tomographic images are reconstructed from the clinical case to show the apices of the interleaflet triangles facing each other between the aortic and pulmonary root (**arrowheads**). This structure is relevant to catheter ablation of ventricular arrhythmia, transcatheter aortic valve intervention, and transcatheter pulmonary valve intervention.

FIGURE 8 Septal Branches of the Left Anterior Descending Artery

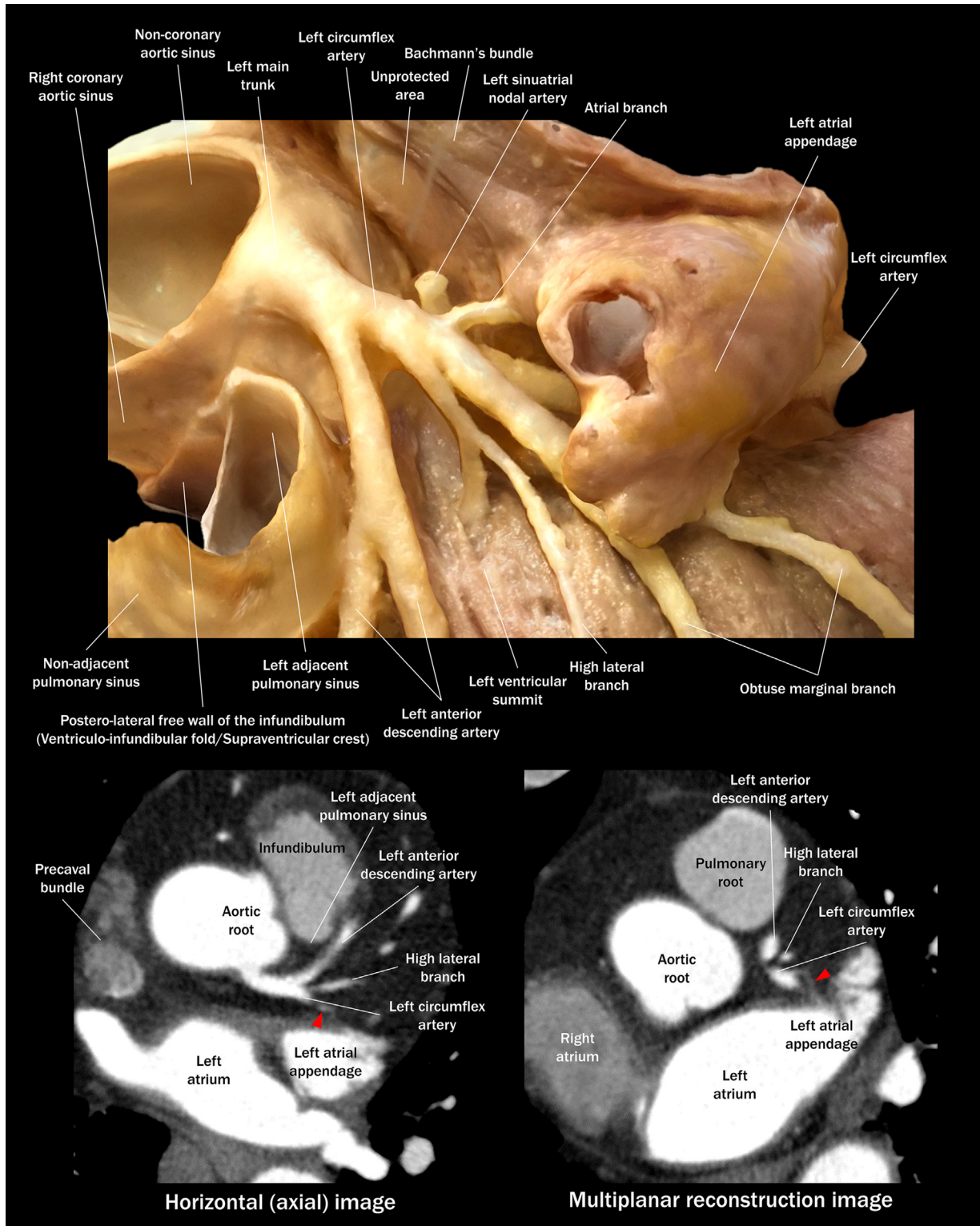


The model is viewed from the frontal direction. This case shows dual left anterior descending arteries (Figure 2). From the medial one running along the anterior interventricular groove, multiple septal branches originate and dive into the groove. The proximal left anterior descending artery is located posterior to the pulmonary root, and the left main trunk is located postero-superior to the pulmonary root.⁴ The left circumflex artery is covered by the left atrial appendage. (Bottom) The cardiac computed tomographic images are reconstructed from the clinical case to show the septal branches of the left anterior descending artery (arrowheads). These structures are relevant to percutaneous coronary intervention, percutaneous transluminal septal myocardial ablation, and catheter ablation of ventricular arrhythmia.

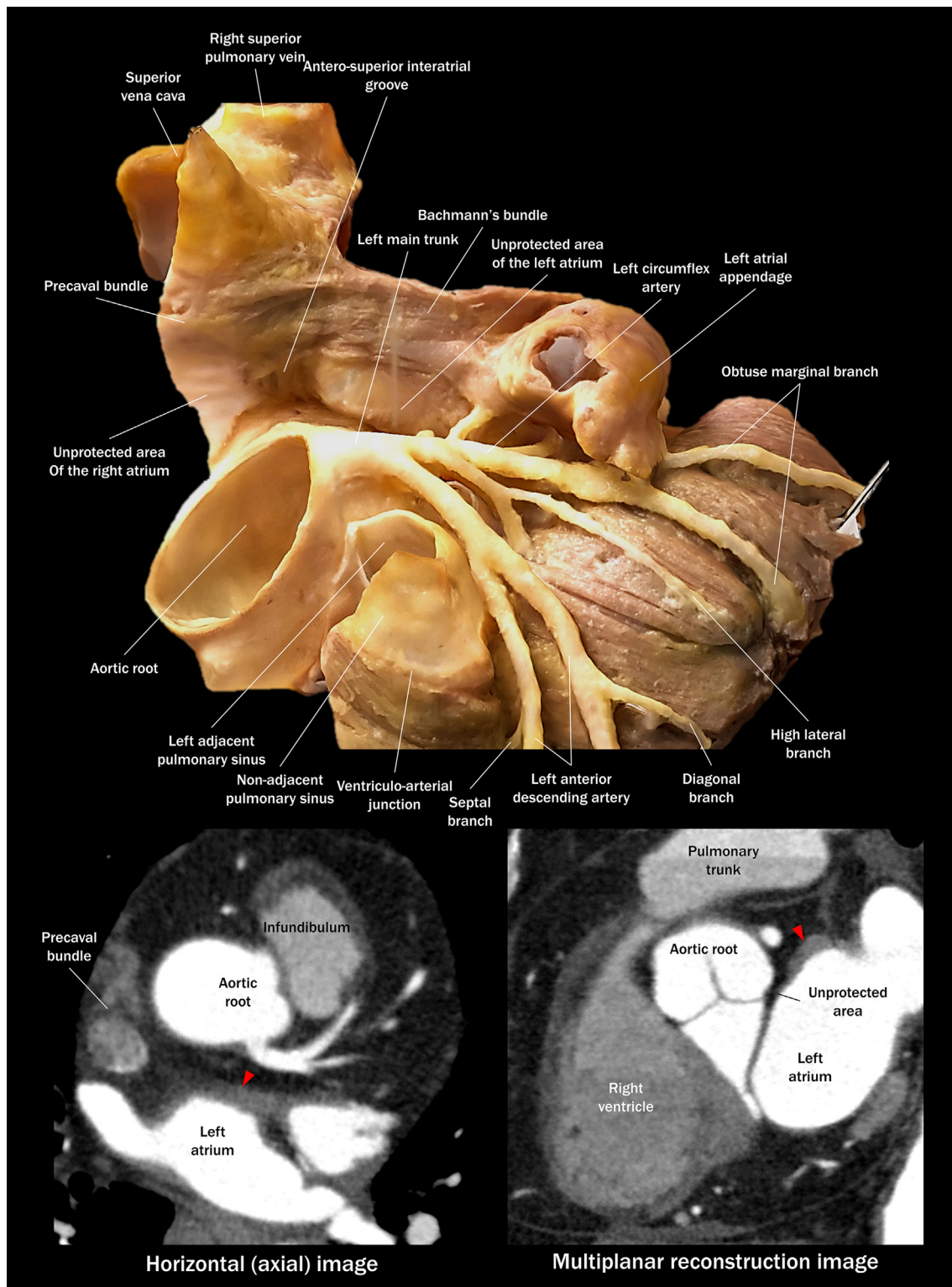
FIGURE 9 Left Ventricular Summit

The model is viewed from the left anterior oblique and cranial direction. The basal superior free wall of the left ventricle, referred to as the left ventricular summit, is covered by the proximal left coronary artery. The compartment above the left ventricular summit is referred to as the left coronary fossa.⁵ It is floored by the left ventricular summit, contains the proximal left coronary artery, is roofed by the pulmonary trunk, and walled by the pulmonary root anteriorly, left coronary aortic sinus medially, anterior wall of the left atrium posteriorly, and left atrial appendage laterally.⁴ The left ventricular free wall muscle at the medial part of the left ventricular summit supports the anterior part of the left coronary aortic sinus. **(Bottom)** The cardiac computed tomographic images are reconstructed from the clinical case to show the left ventricular summit (**arrowheads**). This structure is relevant to catheter ablation of ventricular arrhythmia and transcatheter aortic valve intervention.

FIGURE 10 Left Coronary Artery at the Left Ventricular Summit

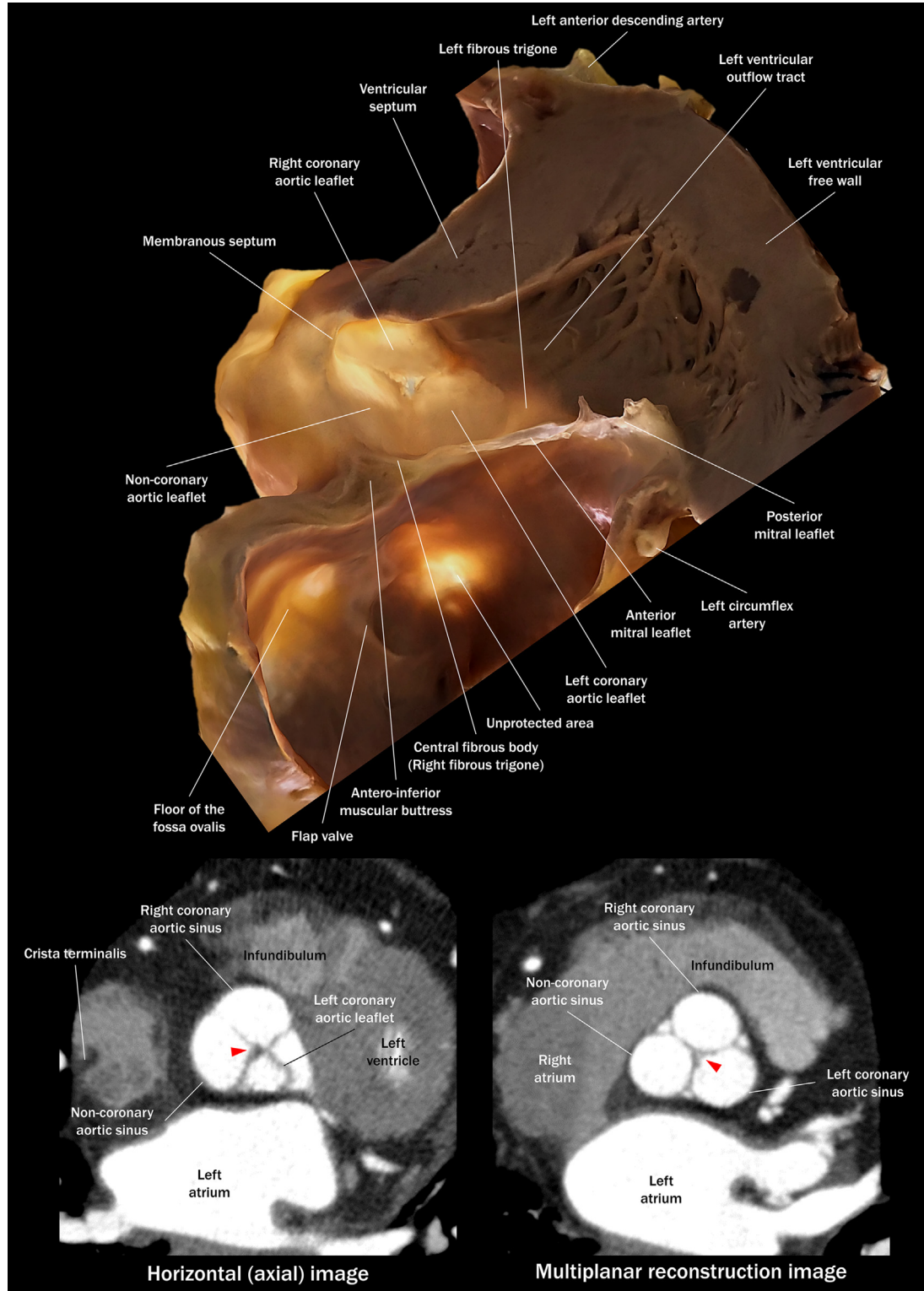


The model is viewed from the left anterior oblique and cranial direction. The left main trunk is located postero-superior to the sinotubular junction of the pulmonary root. The left anterior descending artery skirts the pulmonary root.⁴ Multiple branches of the left circumflex artery can be clearly seen. The left atrial appendage covers parts of these branches. **(Bottom)** The cardiac computed tomographic images are reconstructed from the clinical case to show the atrial branch related to the left atrial appendage (arrowheads). This structure is relevant to percutaneous coronary intervention, percutaneous pulmonary valve/trunk intervention, percutaneous left atrial appendage intervention, and catheter ablation of ventricular arrhythmia.

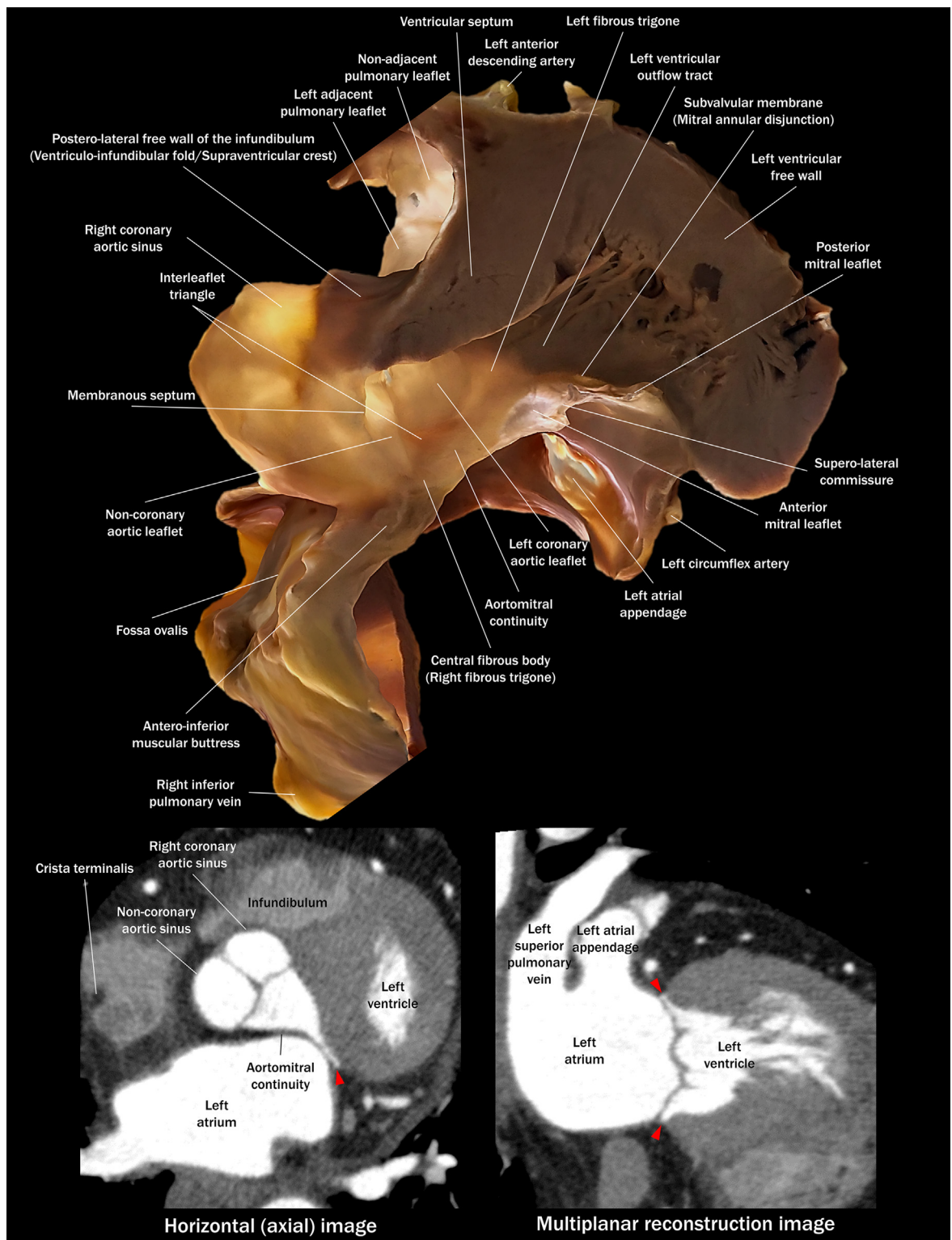
FIGURE 11 Bachmann's Bundle and Unprotected Area of the Atria

The model is viewed from the shallow left anterior oblique and cranial direction. The Bachmann's bundle is the thick subepicardial interatrial muscular connection located at the superior part of the anterior wall of the left atrium. It continues from the precaval bundle, which is also connected with the crista terminalis. The left aspect of the bundle separates at the base of the left atrial appendage. **(Bottom)** The cardiac computed tomographic images are reconstructed from the clinical case to show the Bachmann's bundle (**arrowheads**). These structures are relevant to catheter ablation of atrial arrhythmia and Bachmann's bundle pacing.

FIGURE 12 Aortic Valve Viewed From the Left Ventricular Outflow Tract

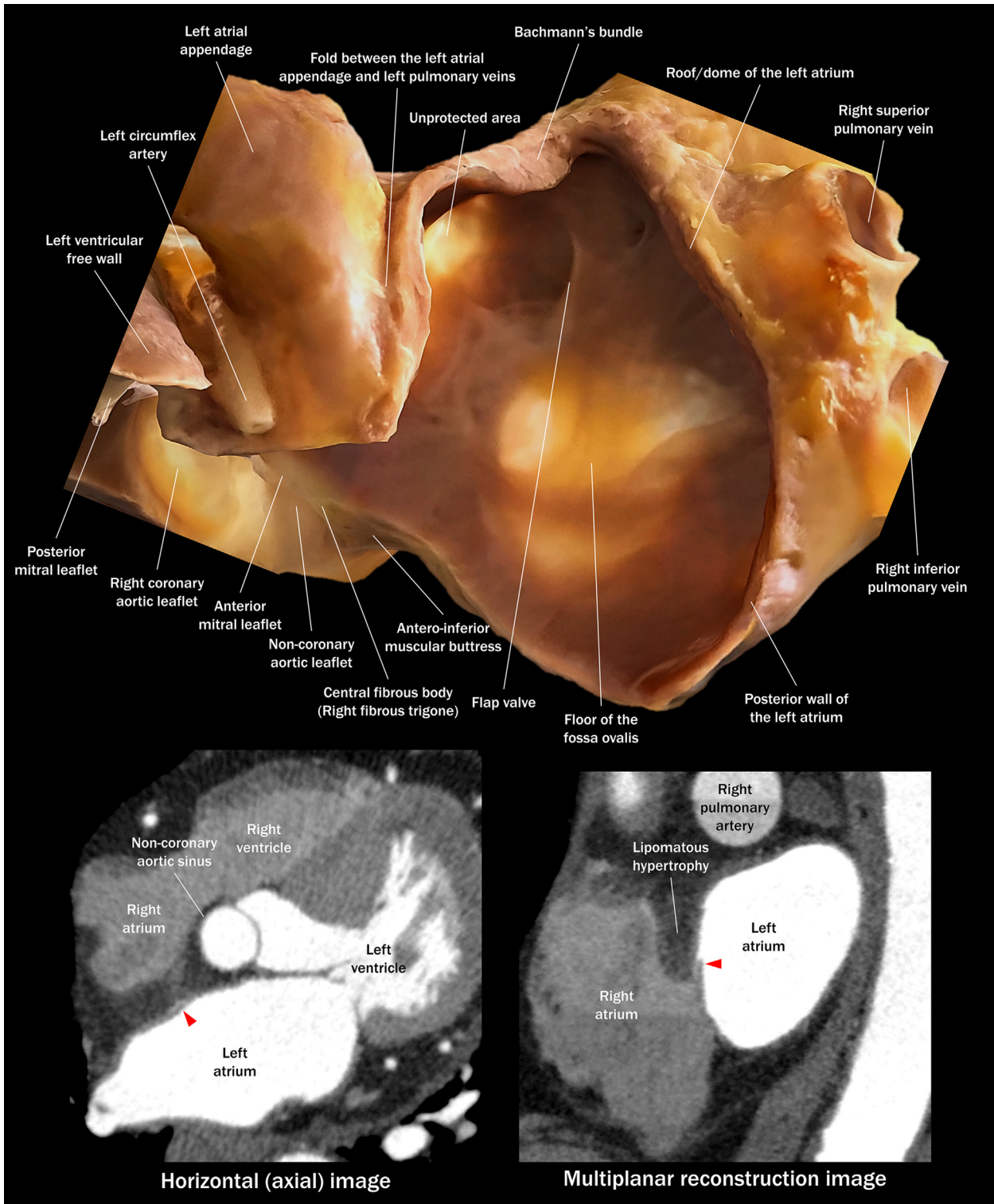


The model is viewed from the right anterior oblique and caudal direction. The right coronary aortic sinus and anterior half of the left coronary aortic sinus are supported by the left ventricular muscle. The rest of the aortic sinuses are supported by the fibrous structures, including the membranous septum, right fibrous trigone (central fibrous body), aortomitral continuity (Figure 13), and left fibrous trigone.⁴ This aspect of the aortic valve is the reason why the aortic valve is often referred to as the “cusp” because this looks like a dental cusp of a molar. (Bottom) The cardiac computed tomographic images are reconstructed from the clinical case to show the central zone of coaptation of the aortic valve (arrowheads). This structure is relevant to transcatheter aortic valve intervention, transcatheter mitral valve intervention, and catheter ablation of ventricular arrhythmia.

FIGURE 13 Left Fibrous Trigone and Subvalvular Membrane

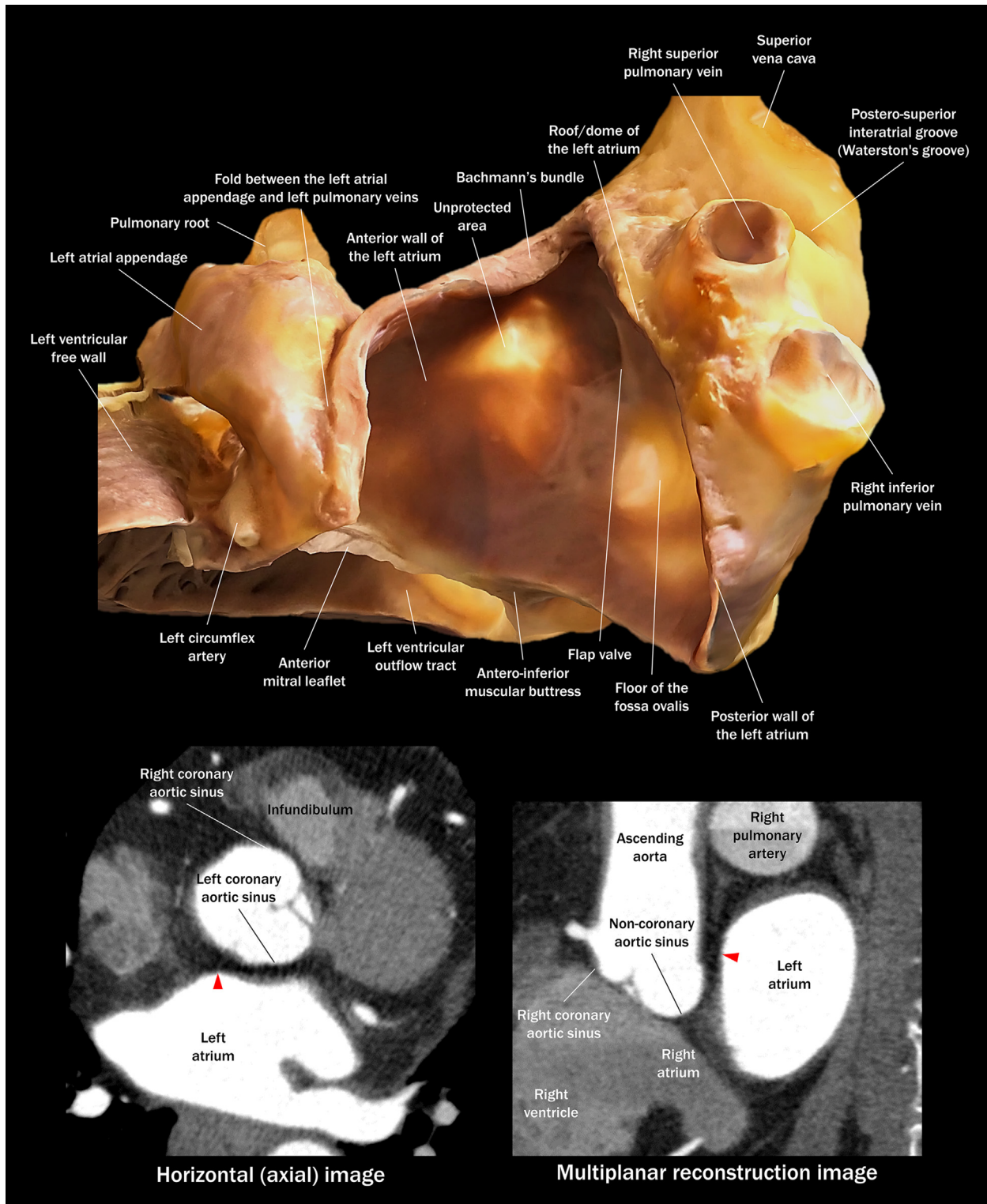
The model is viewed from the caudal direction. The nadir of the left coronary aortic sinus is supported by the left fibrous trigone, a thick fibrous structure connecting the left coronary aortic sinus, anterior mitral leaflet, and the left ventricular free wall muscle. The distal end of the triangle is close to the supero-lateral commissure of the mitral valve and continues to the subvalvular membrane, also referred to as the mitral annular disjunction, where a thin fibrous layer separates the attachment of the posterior mitral leaflet from the left ventricular muscle.⁴ (**Bottom**) The cardiac computed tomographic images are reconstructed from the clinical case to show the subvalvular membrane (**arrowheads**). These structures are relevant to transcatheter mitral valve intervention and catheter ablation of atrial arrhythmia/ventricular arrhythmia/accessory pathway.

FIGURE 14 Flap Valve and Left Side Aspect of the Fossa Ovalis



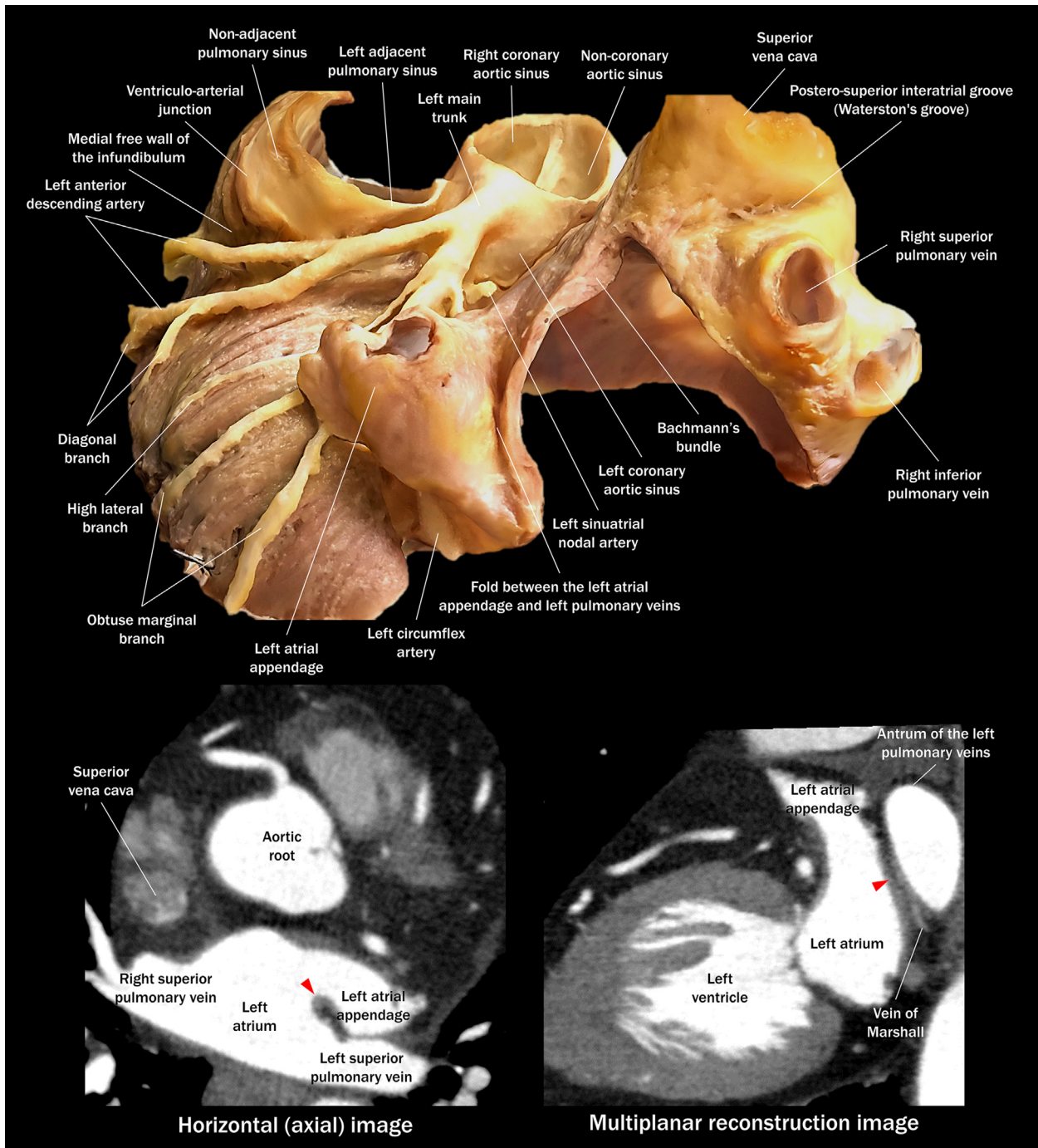
When viewed from the left atrial side, the floor of the fossa ovalis can only be appreciated with transillumination. The opening of the flap valve generally directs antero-superiorly toward the aortic root, and the edge of the flap valve shows an arcuate shape.⁴ In a case with patent foramen ovale, this flap valve is the exact location of the communication between the left and right atria. **(Bottom)** The cardiac computed tomographic images are reconstructed from the clinical case to show the flap valve (arrowheads). These structures are relevant to atrial trans-septal catheterization, catheter ablation of atrial arrhythmia, and transcatheter closure of patent foramen ovale.

FIGURE 15 Unprotected Area of the Left Atrium



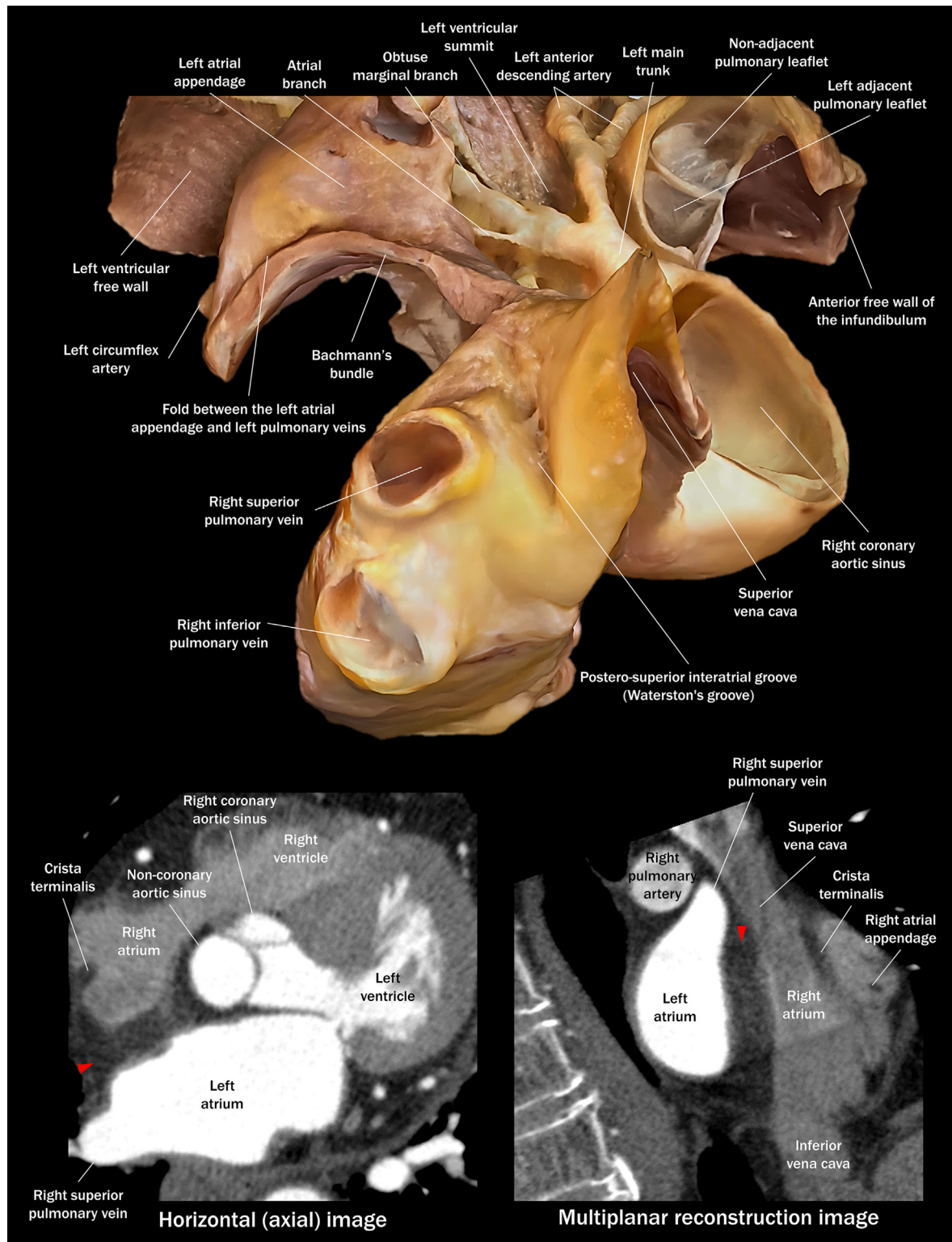
When viewed from the left atrium, the unprotected area of the left atrium (Figure 11) can be appreciated with transillumination. This thin region is located inferior to the Bachmann's bundle and faces to the aortic root.⁴ (Bottom) The cardiac computed tomographic images are reconstructed from the clinical case to show the unprotected area of the left atrium (arrowheads). This structure is relevant to catheter ablation of atrial arrhythmia.

FIGURE 16 Fold Behind the Left Atrial Appendage



A substantial part of the roof and left atrial posterior wall as well as the left pulmonary veins are removed, and the model viewed from the postero-superior direction. The fold between the left pulmonary veins and left atrial appendage is the location of the vein/ligament of Marshall, or the persistent left superior vena cava draining into the coronary sinus. The fold, when viewed from the left atrium, is referred to as the warfarin ridge (coumadin ridge, left atrial ridge).⁴ (Bottom) The cardiac computed tomographic images are reconstructed from the clinical case to show the fold between the left atrial appendage and left pulmonary veins (arrowheads). Note the vein of Marshall running within the fold. These structures are relevant to catheter ablation of atrial arrhythmia, ethanol injection into the vein of Marshall, and percutaneous left atrial appendage intervention.

FIGURE 17 Postero-Superior Interatrial Groove



The model is viewed from the right posterior oblique and cranial direction. The postero-superior interatrial fold between the superior vena cava and right pulmonary veins is also known as Waterston's groove or Sondergaard's groove. This groove is one of the access routes to the left atrium without opening the right atrium during mitral valve surgery.⁴ (Bottom) The cardiac computed tomographic images are reconstructed from the clinical case to show the postero-superior interatrial groove (arrowheads). This structure is relevant to catheter ablation of atrial arrhythmia and catheter ablation of ganglionated plexuses/epicardial connection.

FIGURE 18 Three-Dimensional Replications of the Real Heart



Photogrammetric model (**upper**), real heart sample (**bottom left**), and 3-dimensional printing model (**bottom right**) are demonstrated. When compared with the photogrammetric model (upper), note the left atrial appendage is lifted up by a pin in the real and 3-dimensional printing hearts (**bottom**). Refer to [Supplemental FBX file](#), [Supplemental STL file](#), and [Videos 1 and 2](#).

FUNDING SUPPORT AND AUTHOR DISCLOSURES


This work was made possible by support from National Institutes of Health grants OT2OD023848 to Dr Shivkumar and from the UCLA Amara-Yad Project. All authors have reported that they have no relationships relevant to the contents of this paper to disclose.

ADDRESS FOR CORRESPONDENCE: Dr Shumpei Mori, UCLA Cardiac Arrhythmia Center, UCLA Health System, David Geffen School of Medicine at UCLA, Center of Health Sciences, Suite 46-119C, 650 Charles E. Young Dr South, Los Angeles, California 90095, USA. E-mail: smori@mednet.ucla.edu.

REFERENCES

1. Petriceks AH, Peterson AS, Angeles M, Brown WP, Srivastava S. Photogrammetry of human specimens: an innovation in anatomy education. *J Med Educ Curric Dev.* 2018;5:2382120518799356.
2. Titmus M, Whittaker G, Radunski M, et al. A workflow for the creation of photorealistic 3D cadaveric models using photogrammetry. *J Anat.* 2023;243(2):319-333. <https://doi.org/10.1111/joa.13872>
3. Mori S, Hanna P, Bhatt R, Shivkumar K. The atrioventricular bundle: a sesquicentennial tribute to Professor Sunao Tawara. *J Am Coll Cardiol EP.* 2023;9(3):444-447.
4. Mori S, Shivkumar K. Atlas of Cardiac Anatomy. In: Shivkumar K, ed. *Anatomical Basis of Cardiac Interventions.* Vol. 1. Cardiotext Publishing; 2022.
5. McAlpine WA. *Heart and Coronary Arteries: An Anatomical Atlas for Clinical Diagnosis, Radiological Investigation, and Surgical Treatment.* Springer-Verlag; 1975.

KEY WORDS anatomy, imaging, photogrammetry

 **APPENDIX** For supplementals videos, an FBX file, and an STL file, please see the online version of this paper.